



Supplement of

GPS displacement dataset for the study of elastic surface mass variations

Athina Peidou et al.

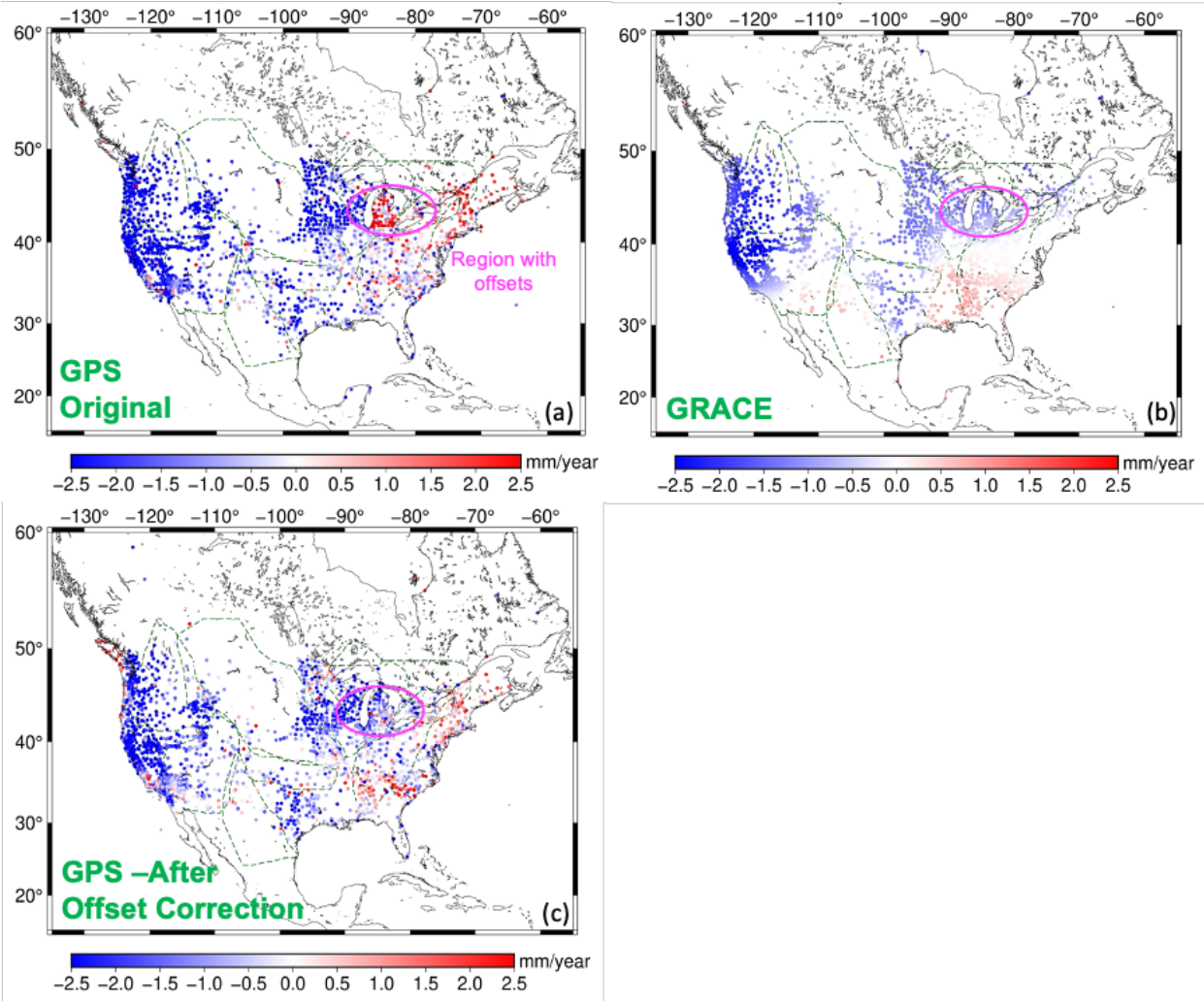
Correspondence to: Athina Peidou (athina.peidou@jpl.nasa.gov)

The copyright of individual parts of the supplement might differ from the article licence.

1 **S1. Offset detection in sites located in Great Lakes region (located at the southwest border part of St.**
2 **Lawrence watershed).**

3 The correlation screening metric showed a significant disagreement between GPS and GRACE(-FO) for sites
4 located in the St. Lawrence basin. The fit between GPS annual signal and GPS/GRACE(-FO) correlation
5 demonstrated a large negative trend $a = -1.26$. The average correlation across the basin was 0.55, which did not
6 reflect a strong negative slope between amplitude and correlation. On top of this observation, another screening
7 metric, trend maps, picked up a flipped trend in sites located in Michigan (part of the St. Lawrence basin) between
8 the period 2015-2018. GPS reflected an uplift while GRACE(-FO) showed a subsidence (Fig. S1a and Fig. S1b).
9 The pronounced disagreement triggered an investigation of the sites timeseries. Sites in Michigan exhibit an abrupt
10 rise of about 7.6 mm and an abrupt east displacement of about 5 mm for about 24 months, starting in April 2016.
11 There were sixty-two stations affected by such a jump. After investigation, we discovered that the issue was in the
12 input NGL data (a mistake in the antenna heights in the header of the rinex files). Once the rinex headers were
13 corrected and the sites were reprocessed, the overall correlation at the St. Lawrence basin improved to 0.61, the
14 extreme negative slope stabilized to $a = -0.2$ (Fig. 2c) and GPS trends over the region aligned with trends picked
15 up by GRACE (Fig. S1c).

Rates estimated between 2015-2018



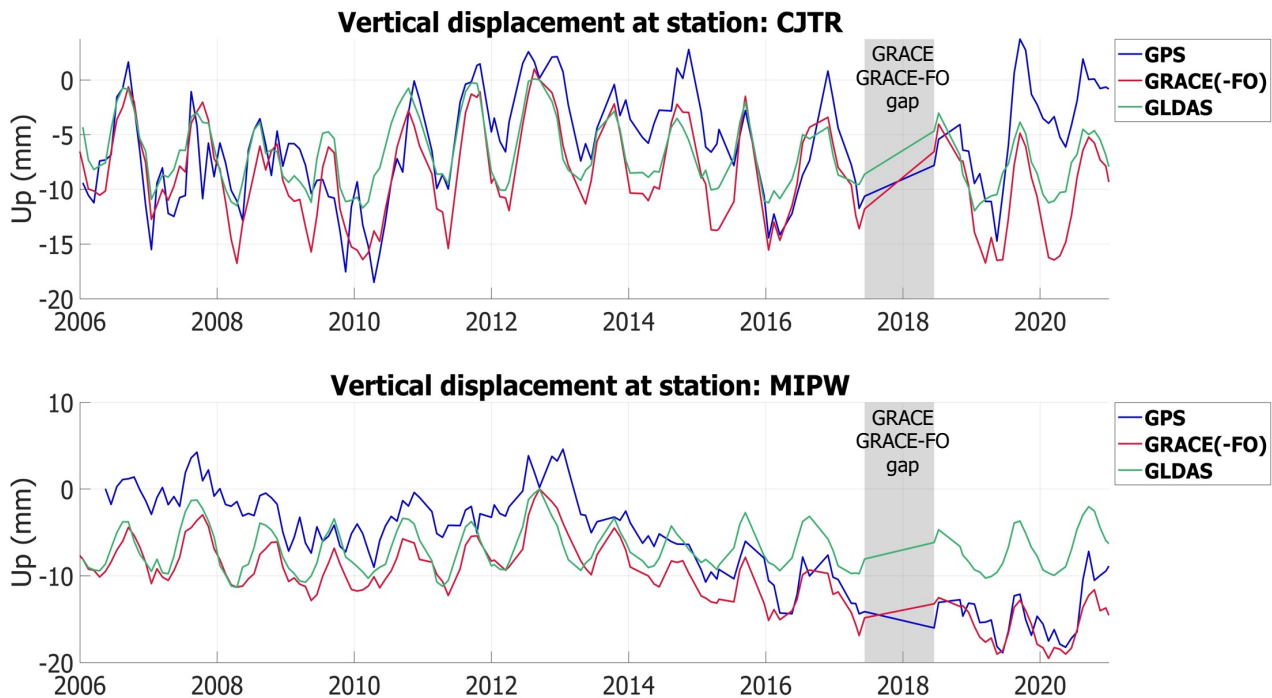
16

17 Figure S1: Rates estimated between 2015-2018 for a) GPS original data (with the unlogged offset); b) GRACE(-
18 FO); and c) GPS after the fixing antenna heights in rinex headers.

19

20

21 **S2. Timeseries of vertical displacements estimated from different techniques, i.e., GPS, GRACE(-FO),**
22 **GLDAS**

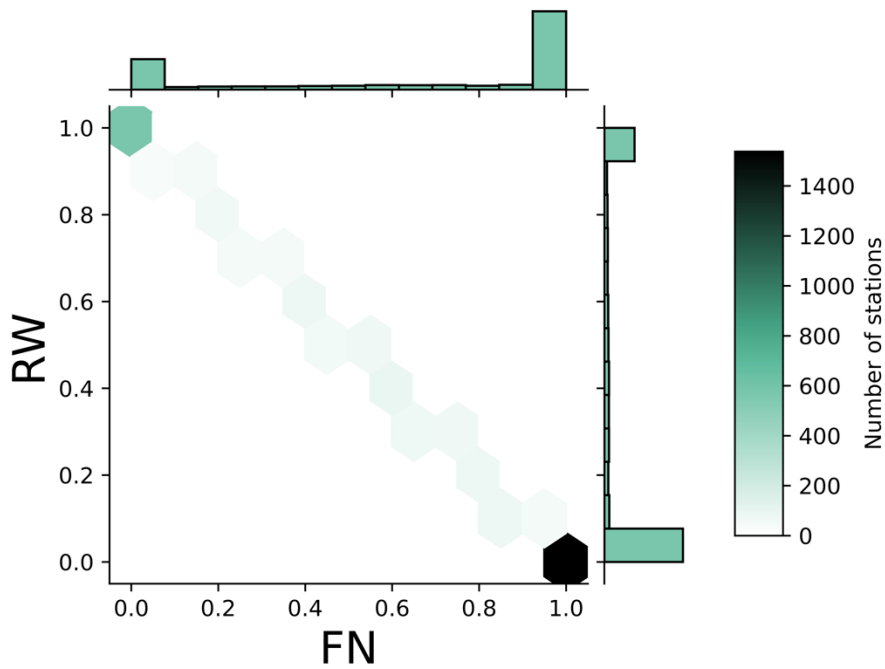


23

24 Figure S2: Timeseries of the vertical displacement (up) for two stations, i.e., CJTR (lon, lat = -92.273, 34.822
25 degrees) and MIPW (lon, lat = -85.657, 42.463degrees). GPS vertical displacements are in blue; GRACE(-FO) in
26 red and GLDAS in green. Note that during GRACE/GRACE-FO gap (shaded grey area) there are no records.

27 **S2. Relative contribution of Flicker Noise and Random Walk Noise to WN+FN+RW**

28 When all three noise models are considered, we notice that white noise does not describe even minimally the noise
29 of the GPS timeseries residuals. It is flicker noise and random walk the two noise models that describe the total
30 uncertainty of the estimates. We performed a detailed analysis to understand the structure and the contribution of
31 each of the two noise models to the total noise. Hector software provides the fraction (percentage) contribution,
32 which we plot on S3. The contribution of a noise model to the total noise estimated to describe the uncertainty of
33 a GPS timeseries ranges between [0 1]. Almost half of the stations' noise is described exclusively from flicker
34 noise (dark green point centered at $x, y = 1.0, 0.0$) and one fifth of the datasample (600 stations) are described
35 exclusively by random walk noise (green point centered at $x, y = 0.0, 1.1$) and from random walk for 600 stations.
36 Residuals of the rest of the stations (~ 800) demonstrate noise characterized by a combination from both noise
37 models shown (see S3).



38

39 Figure S3: Diagram representing the contribution of random walk and flicker noise to a combined WN+FN+RW
 40 uncertainty quantification. The percentage contribution of FN is shown on x-axis and of RW on y-axis. Color
 41 variations denote the number of stations exhibiting the percentage contribution. A histogram with the number of
 42 stations is also plotted at the x and y-axes.